Towards fuel spray ignition in aircraft engine

A. Bruyat*, G. Linassier, P. Villedieu, N. Bertier, O. Rouzaud, R. Lecourt, G. Lavergne
ONERA-The French Aerospace Lab, F31055 Toulouse, France,
TURBOMECA-Safran group, Bordes, France
ONERA-The French Aerospace Lab, F92322 Châtillon, France
ONERA-The French Aerospace Lab, F31410 Mauzac, France

Abstract

The present study aims at contributing to the development of a methodology to predict and improve the ignition performances of industrial combustors. A model has been developed to investigate the early growth of a spherical ignition kernel in a two-phase flow mixture. It is combined with a multiphysic code, with two different approaches. RANS and LES simulations have been performed on an experimental combustion chamber with a swirl injector, reproducing one sector of an industrial combustor. The gas and spray behavior have been validated. The ignition kernel model is used to build the ignition probability map of a combustor from the mean and instantaneous flow fields.

Introduction

Spray ignition represents one of the key parameter in the design of turbojet combustors. In case of in-flight extinction, relight must be possible, even for high altitude conditions. For helipad engines, cold engine start-up at high altitude is also necessary for mountain rescue. At altitude higher than 6000 m, pressure is lower than 0.5 bar and air, engine parts and fuel temperatures are as low as 233 K. These conditions are critical for engine relight, because of the degradation of spray atomization quality and the difficult vaporization process.

For air-breathing engines, the most reliable and common ignition mode is an electrical spark discharge, which efficiently converts electrical energy into a small heat deposit. The ignition process is constituted of two main phases, ignition kernel formation and kernel propagation [1], [2]. Kernel formation can be divided in two steps: energy deposition (spark discharge) and spherical flame expansion (small-scale flame propagation). Kernel propagation also takes place in two different steps: kernel is formed into a recirculation zone and then flame propagates to the whole chamber.

To certify new concept of combustors, numerous and expensive ignition tests are realized over a wide range of conditions. Such tests cannot be afford to the preliminary design phases. An alternative approach is the use of reliable numerical tools which could reduces the overall design cycle.

Nowadays, with the growth of computational performances, LES can be afforded for such purpose. LES offers the advantage to capture the large scale of turbulence, and is suitable to simulate an highly stochastic phenomena like ignition [3] [4], but it still needs great computational cost. Moreover, before performing a time consuming flame propagation simulation, it should be interesting to use a simple methodology to predict ignition of the combustor [5] [6].

An ignition kernel model has been developed and combined with a CFD code in two ways (Figure 1). Firstly, the ignition model is used to build the ignition probability map of a combustor. Secondly, an ignition simulation is introduced as initial condition in an unsteady simulation to model the complete flame propagation [7].

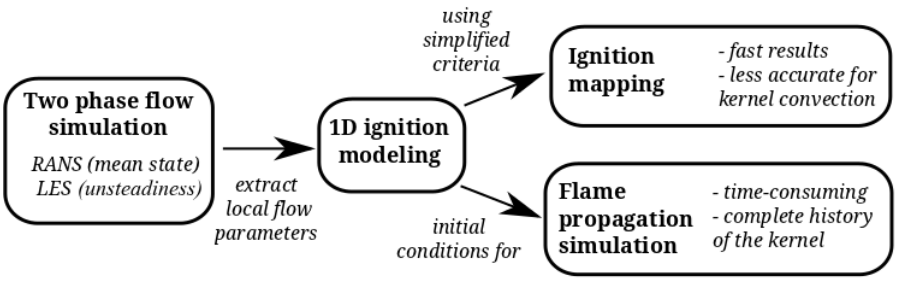

Figure 1. Description of the ignition prediction methodology.

*. Corresponding author: anne.bruyat@onera.fr

Both methodologies are tested on a mono-sector combustor, experimentally applied to the MERCATO test-rig (ONERA-Mauzac). RANS and LES have been performed with unstructured compressible in-house code CEDRE [8]. Spray have been modeled with a Lagrangian approach. Non-reactive simulations have been validated thanks to velocity fields of the two-phase flow and the droplet size fields provided by LDA and PDA measurements. It has been also verified that LES captures correctly the unsteadiness of the gas flow. From RANS two-phase flow field, an ignition probability map and two flame propagation simulations have been studied. Similar simulations are expected to be performed on different LES flow fields.

Prior ignition two phase flow simulation

Two phase flow solver

Gaseous solver

The unstructured compressible code CEDRE have been used for both RANS and LES, with an implicit time advancement, and a second-order upwind scheme. For RANS approach, the kinetic energy is modeled with the standard k-l model, with an inlet turbulent rate set to 5 %. For LES, the Smagorinsky model has been used to model the subgrid scales. A non-reflecting condition was considered for the exit of the combustor since the exit is far enough.

Dispersed phase solver

The liquid phase is modeled using a Lagrangian approach. Two-way coupling is considered for liquid-gas interactions. Kerosene is represented by the surrogate component $C_{10}H_{20}$. An infinite conductivity model was used to predict the evaporation of the droplets, and the Ranz-Marshall correlations are used to modify the Nusselt and Sherwood numbers. For RANS simulations, the turbulent dispersion is taken into account with a Langevin model. The instationnary aspect of LES make the use of such model unnecessary. A complex treatment is applied to the walls. Depending on their properties (temperature, Weber number), the droplets will bounce at the wall, or splash [9].

Test case description

Geometry

The test case is a mono-sector combustor with square section, and can be seen on Figure 2. Dimensions of the combustion chamber are $130 \times 130 \times 250 mm^3$. The injection system, designed by Turbomeca, is composed of a pressure atomizer and an air swirler. The complete test-rig includes a plenum and an exhaust pipe, which are also meshed, so the flow inside the injection system is also modeled. A spark plug device can be mounted on the lateral wall, at four different locations (26, 56, 86 and 116 mm) from the bottom wall of the combustion chamber.

For the present study, all simulations have been performed for the following operating conditions : $Q_{air} = 35.0\,\mathrm{g{\cdot}s^{-1}}$, $Q_{kero} = 2.25\,\mathrm{g{\cdot}s^{-1}}$, $P = 1\,\mathrm{bar}$ and $T = 293\,\mathrm{K}$. The global equivalence ratio Φ is equal to 0.95. For these operating conditions, the combustor have been thoroughly experimentally characterized on the MERCATO facility, at ONERA[10].

For flame propagation, two spark plug positions have been tested, located at 56 mm and 116 mm. Ignition tests for 56 mm abscissa gave ignition with a probability $P_{ign} = 37\,\%$ [11]. For 116 mm position, ignition is not possible for this global equivalence ratio.

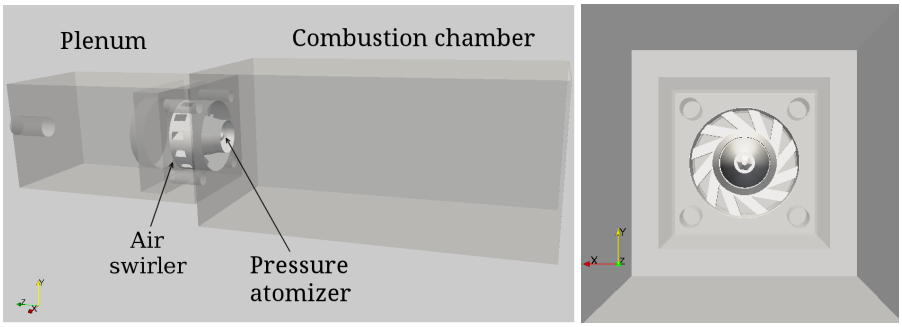

Figure 2. Schematic view of the MERCATO combustion chamber.

Injection modeling

Fuel is injected downstream the injector nozzle, as an ensemble of injection points divided as rings. Injection profile is defined from particle granulometry and velocimetry measurements, obtained with a two-component PDA system, at the 6 mm section, so as the dispersed flow is ensured. Polydisperse effects are taken into account, by injecting ten classes of droplets size and respecting size and velocity distributions.

In the RANS case, the fuel is injected at the measurement section. With LES, injection is done at the bottom wall of the chamber, that is to say at 4 mm from the injector. This is done in order to take into account effects of the swirl on the droplets from the early instants. Granulometry is conserved, since the temperature is low ($T = 293\,\mathrm{K}$) evaporation is neglected.

Results for cold flow

Gaseous phase

For LES and RANS, velocity fields of the gas phase have been compared to experimental data obtained with a two-component LDA device. These measurements are not available for the simulated operating conditions, but previous works showed that the mean and RMS velocities are self-similar, and can be normalized with the air bulk velocity. For the current study, we used operating conditions for which the bulk velocity is 10 % lower than the one of our test case. LES results are averaged over 120 ms. For both LES and RANS simulations, the mean velocity profiles show good agreement with the measured ones. The LES approach gives better results for RMS value levels, whereas RANS simulation tends to underestimate the kinetic turbulent energy. This tendency have been previously observed in other works on swirling flow [12].

The experimental pressure loss between plenum and the combustion chamber was measured to approximately $\Delta P_{exp} = 5300\,\mathrm{Pa}$. The LES simulation gives $\Delta P_{LES} = 4500\,\mathrm{Pa}$, and RANS simulation gives $\Delta P_{RANS} = 4300\,\mathrm{Pa}$.

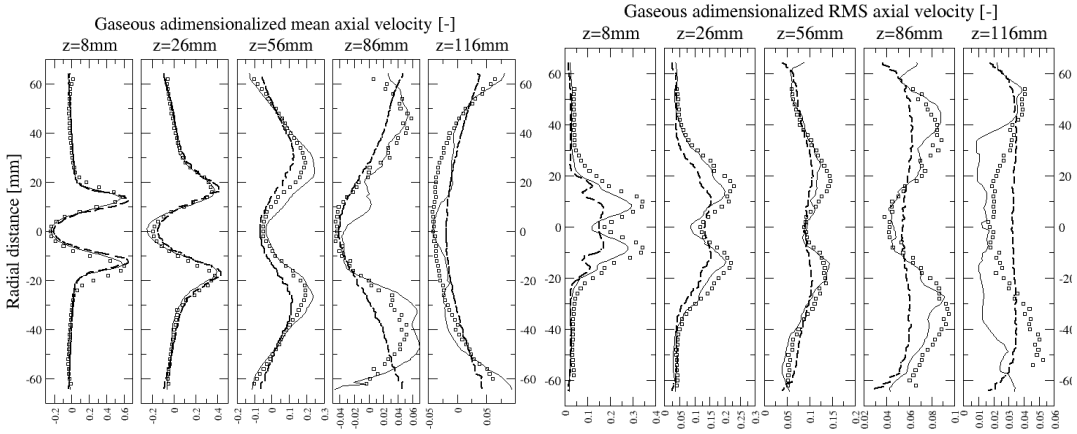

Figure 3. Simulation of the cold flow (□: LDA,– : LES ,−− : RANS).

Dispersed phase

The validation of the two-phase flow is difficult, since only few experimental data on the simulation operating conditions are available. Size and velocity distributions have been measured only at the 6 mm section. Axial droplets velocities and the flow rate are presented on Figure 4. Simulations are in good agreement with experiments, as for the other velocity components. LES and RANS normalized flow rates profiles are slightly different. Both of them show a high flow rate in the vicinity of the walls which was experimentally observed.

With an high enough bulk velocity, rotationnary flow exhibits an hydrodynamic instability called Precessing Vortex Core [13]. Spectra pressure was obtained using a microphone for non-reactive conditions [10]. On Figure 5, spectral density of experiments and LES calculations are compared. For both of them, maximum spectral density indicates the frequency of the hydrodynamic instability, which is 985 Hz for LES and 1050 Hz for experiments. The discrepancy between these results is slight. Acoustic frequencies of the combustion chamber are also well defined. The structure of double-helix of the PVC can also be observed from LES unsteady flow field, on Figure 5. As seen on experimental visualization and on numerical investigations, the PVC strongly interacts with droplets in the vicinity of the injector. This behavior is well captured by LES at the 26 mm section plotted on Figure 5. An analysis shows that particles which rotate with the PVC, on the center of the section, are small droplets caught

in the central recirculation. This interaction is not observed at the 6mm section, which may be due in part to the delayed injection of 4mm from the injector. At this section plotted on Figure 6, the recirculating droplets of the non-reactive flow are influenced by the recirculating zones in the corners of the chamber and have a low velocity, whereas droplets newly injected have a high axial velocity. Isolines of gaseous instantaneous axial velocity are plotted to underline this behavior.

Sparks are located near the wall, and it is interesting to know if the local liquid volume fraction has a periodic behavior. A laser tomography is experimentally performed at different points. The analysis captures the PVC frequency in the main jet, but no coherent structure is detected near the sparks. The unsteady gaseous mass fraction of the flow is investigated with LES and it leads to the same conclusion: although the spray has an unsteady behavior near the walls, it is not led directly by the PVC.

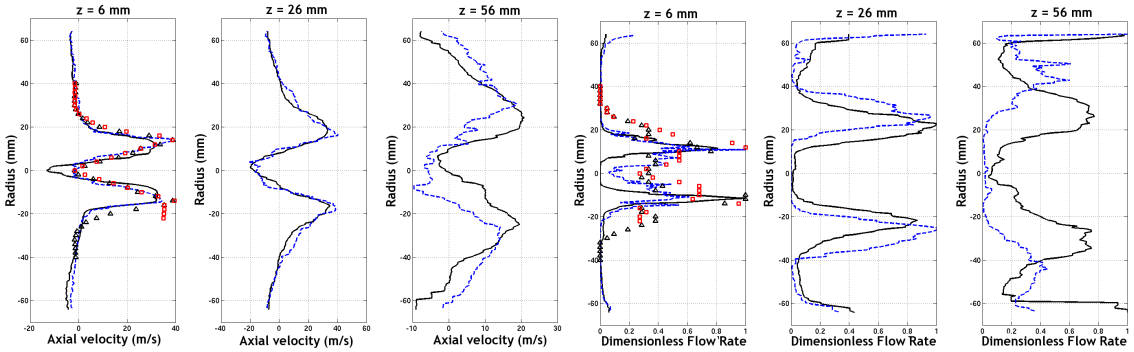

Figure 4. Simulation of the two-phase flow (□ and △: PDA,- : LES ,−− : RANS) : a) Axial velocity, b) Dimensionless Flow Rate

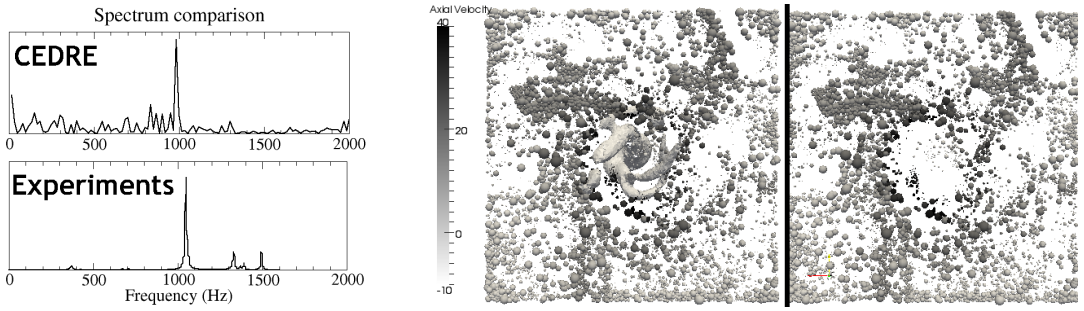

Figure 5. a) Spectra pressure from LES and experiment, b) Interaction of the spray with the PVC, at section z =26 mm, droplets colored by their axial velocity

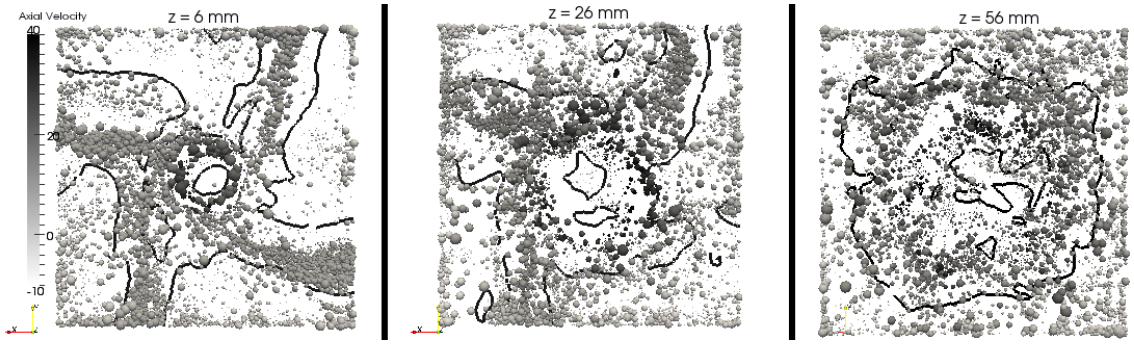

Figure 6. Clip of an instantaneous two-phase flow field, droplets colored by their axial velocity, and isolines of gaseous axial velocity $V^g_{axi} = 0$

Ignition modeling

Ignition kernel model

The aim of the present model is to simulate the early propagation of an ignition kernel in a two-phase mixture [14], [15]. The energy deposit is considered as an instantaneous, adiabatic and isobaric heating process, which creates a spherical laminar flame front. On the first stage of ignition, it is assumed that the flame front is not wrinkled by turbulence. With these hypothesis, the kernel growth phase is described by numerical resolution of conservation equations for 1D dilute-spray mixture. In spherical coordinates, it gives the equations 1, 2 and 3, with the source terms $\dot{\rho}_{i,\chi}$ and $\dot{\mathcal{H}}_\chi$ for chemical reactions, and $\dot{\rho}_{l,v}$ and $\dot{\mathcal{H}}_v$ for fuel evaporation.

$$\frac{\partial \rho_g}{\partial t} + \frac{1}{r^2}\frac{\partial}{\partial r}\Big(r^2 \rho_g\, u_{r,g}\Big) = \dot{\rho}_{l,v} \tag{1}$$

$$\rho_g \frac{\partial Y_i}{\partial t} + \rho_g\, u_{r,g}\frac{\partial Y_i}{\partial r} - \frac{1}{r^2}\frac{\partial}{\partial r}\Big(r^2 \rho_g \mathcal{D}_{i,g}\frac{\partial Y_i}{\partial r}\Big) = \dot{\rho}_{l,v}(\delta_{i,\mathrm{F}} - Y_i) + \dot{\rho}_{i,\chi} \tag{2}$$

$$\rho_g c_{p_g}\frac{\partial T_g}{\partial t} + \rho_g c_{p_g} u_{r,g}\frac{\partial T_g}{\partial r} - \frac{1}{r^2}\frac{\partial}{\partial r}\Big(r^2 \lambda_g \frac{\partial T_g}{\partial r}\Big) = \dot{\mathcal{H}}_v - \dot{\rho}_{l,v} h_{l,(g)} + \dot{\mathcal{H}}_\chi \tag{3}$$

Droplets are described by a Lagrangian approach. The displacement of the droplets is neglected during kernel simulation. Evaporation is modeled with a d^2-law using an infinite-conductivity model, with Ranz-Marshall correlations.

Experimentally, he energy deposit takes place in a spherical volume of radius r_0, close to the spark plug air-gap. Numerically, ignition kernel simulation starts after the kernel has expanded to a radius $r_1 > r_0$. The initial radius r_1 and temperature T_1 are calculated with kernel visualization and the energy of the spark discharge [2]: $r_1 = 5.1\,\mathrm{mm}$ and $T = 3500\,\mathrm{K}$. It corresponds to the energy after a energy loss of 50 %, during the spark generation, of the electrical energy supplied to the spark plug.

Is is also assumed that the kernel expansion takes place in a quiescent mixture. In order to fulfill this hypothesis, the ignition simulation time has been set as the time necessary for the kernel to move of his diameter. This time has been measured experimentally.

Combustion is modeled using a reduced two-step chemical scheme (equation 4) [16]. The chemical reaction rate is calculated with an Arrhenius law, with a correction of the pre-exponential factor depending on the local equivalence ratio. Fuel is modeled with a monocomponent component, referred as $\mathrm{C_{10}H_{20}}$ [16]:

$$\mathrm{C_{10}H_{20}} + 10\cdot\mathrm{O_2} \rightarrow 10\cdot\mathrm{CO} + 10\cdot\mathrm{H_2O} \qquad \textit{and} \qquad \mathrm{CO} + \frac{1}{2}\cdot\mathrm{O_2} \leftrightarrows \mathrm{CO_2} \tag{4}$$

The kernel model is used to perform quick analysis of a combustor ignition, from an instantaneous or mean flow field. Local ignition of the spray occurs if the produced fuel vapour is within the flammability limits and if the energy deposit is high enough to enable combustion (*Condition 1*). This ignition can be detected by a local maximum on the mean temperature of the kernel (Figure 7). Then, growth of the kernel is analysed to eliminate positions where no propagation of the kernel flame front occurs (*Condition 2*). Final mean temperature of the kernel is examined, to garantee the flame front sustained (*Condition 3*).

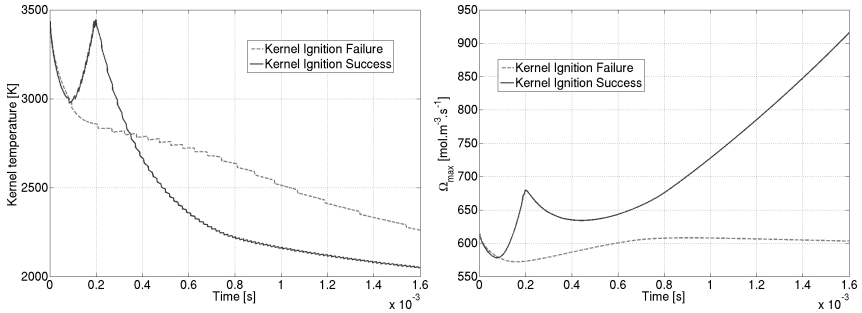

Figure 7. Time evolution of the mean kernel temperature and of the maximum reaction rate during ignition simulation.

If the three conditions for local ignition are fulfilled, the propagation of the flame to the injector is predicted using a simplified propagation criterion (*Condition 4*)(Figure 8), inspired from [17], based on the comparison of the turbulent flame speed S_T to the axial velocity component u_{axi} :

1. $S_T > u_{axi}$: the kernel is advected toward the injector, and the flame spreads to the whole combustor,
2. $S_T \leq u_{axi}$: the kernel is advected toward the combustor exit, and ignition is not possible.

with the turbulent flame speed S_T, calculated for a stoechiometric gaseous mixtue like $S_T = S_L^0 + u'$ [18]. This condition is directly applied to the LES unsteady flow. From RANS turbulent variables, the probability of upstream propagation of the kernel $P_{up} = P(S_T > u_{axi})$ can be computed at the kernel deposit location. With the assumption that u' follows a normal law, P_{up} can be expressed as in equation 5, from the mean velocity $\overline{U}$:

$$P_{up} = \frac{1}{2} \cdot \left[\text{erfc} \left(\frac{-S_T + \overline{U}}{u'\sqrt{2}} \right) \right] \tag{5}$$

This is not sufficient to describe the complex trajectory of the kernel, but it can be used to discriminate locations where upstream flame propagation is not possible at all.

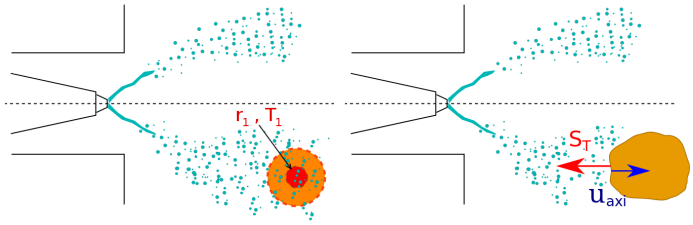

Figure 8. Ignition mapping criteria : on the left, one-dimensionnal simulation of the laminar kernel growth ; on the right, criteria on the flame kernel propagation to the injector nozzle.

Results and discussion

Ignition mapping

The described methodology has been first applied to the RANS steady flow field. Figure 9 shows the successive steps to identify locations with good ignition probability. The analysis of the kernel temperature is not shown here, because the temperature of the kernel remains above 2600 K in the whole area tested. Is shall be noticed that this criteria is more relevant in the case of low-temperature flow, or in the LES unsteady case.

On Figure 9.a is plotted the local inflammation detection of the kernel from RANS simulations. The Figure 9.b shows the growth of the ignition kernel after the ignition simulation. Ignition and kernel growth are possible in region with strong liquid concentration: on the spray cone and in the vicinity of the wall. After the impact of the spray on the wall, part of the droplets is recirculated by the flow in the lateral zone. The gas flow also exhibits a central recirculation zone, but droplets recirculation in this zone does not provide enough fuel to enable ignition. The probability of upstream propagation is drawn on Figure 9.c. Two zones of low P_{up} can be identified : one corresponds to the high velocity zone of the jet, the other is located near the wall, downstream from 80 mm abscissa.

Finally, Figure 9.d shows a scatter plot of ignition kernels allowing ignition of the combustor for which the following limiting parameters for ignition have been chosen : the total equivalence ratio $\phi_{glob} > 0.4$, $\frac{r}{r_1} > 1.15$ to ensure the kernel has grown sufficiently, $P_{up} > 0.6$ to ensure the flame speed is higher than the gaseous axial velocity, and finally $T_{kernel} > 600\,\text{K}$ so that the kernel is hot enough to be able to vaporizes droplets and combustion.

Since the droplet volume fraction seen by sparks varies over time, the unsteady flow fields obtained by LES are investigated. The methodology is applied on several instantaneous flow fields. They are investigated with a 10000 Hz frequency over a total time of 9 ms, so that the 1000 Hz PVC cycle is well-defined. The propagation criterion $S_T > u_{axi}$ is simply applied to the unsteady flow fields. The number of realized ignition over the total number of realisations leads to the ignition probability plotted on Figure 10.

The ignition maps, plotted for the upper part of the combustor, show that ignition is highly probable in the corner recirculation zones, and particularly at the 26mm spark, but it is low in the central recirculation zone. This is in good agreement with experimental results and observations : around the fuel injection axis there are only few droplets, which means the global equivalence ratio is low. The grey experimental data show that ignition is possible though most ignition test fail. LES unsteady flow fields also show that ignition is possible. Ignition probability in the vicinity of the 56mm spark appears to be intermediate. Investigation shows that this result mostly comes from

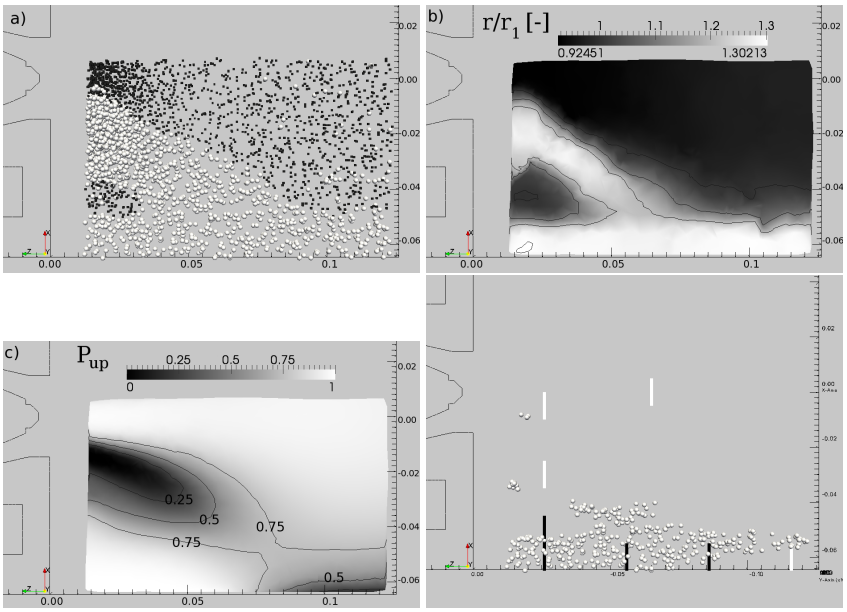

Figure 9. Ignition probability mapping on MERCATO : a) scatter plot of the tested ignition spheres (black square = local ignition failure, white sphere =local ignition success) ;b) growth of the kernel; c) probability of upstream propagation of the flame P_{up} with iso-contour; d) scatter plot of successful global ignition positions from simulation, and experimental results (white line : no-ignition, black line : ignition of the combustor).

the propagation criterion. Finally, one should notice there is no criterion about the rich equivalence ratio, since the spray widen the flammability limits [20]. However, in zones where the equivalent ratio is high, the temperature resulting from the ignition kernel model can be too low (T < 600 K) and there is no ignition. It might then be underlined that these ignition probability results are highly dependent on the chosen limiting parameters.

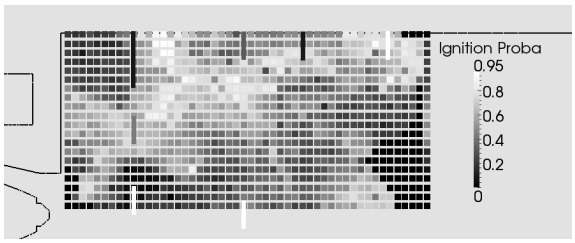

Figure 10. Ignition probability mapping on MERCATO from LES unsteady flow fields (points), compared to experimental data (lines). Experimental data scale is inverted (black = ignition, white = no-ignition)

For abscissa 116 mm, some kernel with successful ignition can be found near the wall, but the flame propagation criterion P_{up} remains lower than inside the recirculation zone, and this region seems to be less favourable to ignition success. Actually, visualisation with high speed camera of the ignition process showed the formation and growth of an ignition kernel in this zone, and seems to indicate that the limiting criterion for ignition success is the flame kernel propagation. It shall be noticed that the exact ignition probability is not reproduced by the ignition mapping, since P_{up} is only locally calculated, and do not take into account the complete trajectory, and possible posterior quenching of the kernel. Still, it is possible to isolate some regions of the flow where the ignition is possible, and to understand some limiting parameters to the phenomena.

Conclusions and perspectives

RANS and LES have been applied to simulate non-reactive two-phase flow of an experimental combustor, with a Lagrangian modeling for the liquid phase. The mean characteristics of the flow are well reproduced by both methods, and LES enables to capture precisely the hydrodynamic instability present for this regime and its interaction with droplets.

From RANS mean flow and from LES instantaneous flow fields, ignition mapping have been tested, and results show good agreements with the main features observed on the combustor during ignition tests. More simulations may lead to the caracterisation of the unsteady ignition process of combustion chambers. Multicomponent effects on the ignitions may be investigated.

Acknowledgements

The authors would like to acknowledge the financial support from Turbomeca, the "Association Nationale pour la Recherche et la Technologie" and the "Direction Générale de l'Armement".

References

[1] Thiele, M., Selle S., Riedel, U., Warnatz, J., and Maas, U., Numerical simulation of spark ignition including ionization. *Proceedings of the Combustion Institute*, Volume 28, pp. 1177-1185 (2000).

[2] García-Rosa, N., *Phénomènes d'allumage d'un foyer de turbomachine en conditions de haute altitude*. PhD Thesis, Université de Toulouse, 2008.

[3] Subramanian, V., Domingo., P., and Vervisch, L., Large eddy simulation of forced ignition of an annular bluff-body burner. *Combustion and Flame*, 157:579-601.

[4] Boileau, M., Staffelbach, G., Cuenot, B., Poinsot, T., and Berat, C., LES of an ignition sequence in a gas turbine engine. *Combustion and Flame*.

[5] Boyde, J., M., Domenico., M., Noll, B., and Aigner, M., Spark ignition simulations and the generation of ignition maps by means of a turbulent flame speed closure approach. *Proceedings of ASME Turbo Expo 2010*, Glasgow, June 2010.

[6] Weckering, J., Sadiki, A. , Janickay, J., and Mastorakos, E., Investigations of ignition probability of a forced ignited turbulent methane jet using LES. *V European Conference on Computational Fluid Dynamics*, Lisbon, June 2010.

[7] Linassier, G., Bruyat, A., Villedieu, P., Bertier, N., Rouzaud, O., Laurent, C., Lecourt, R., Verdier, H., Lavergne, G., RANS and LES simulations of aircraft engine ignition *3rd INCA Colloquim*, 2011.

[8] A. Refloch, B. Courbet, A. Murrone, P. Villedieu, C. Laurent, P. Gilbank, J. Troyes, L. Tessé, G. Chaineray, J.B. Dargaud, E. Quémerais, F. Vuillot, *CEDRE Software*,*The ONERA Journal Aerospace Lab*, Issue 2, March 2011

[9] Garcia Rosa, N., Villedieu, P., Dewitte, J., Lavergne, G., A new droplet wall interaction model. *Proceedings of the ICLASS*, Kyoto, August 2006.

[10] Lecourt, R., Linassier, G., Lavergne, G., Detailed characterisation of a swirled air/kerosene spray in reactive and non-reactive conditions downstream from an actual turbojet injection system. *Proceedings of ASME Turbo Expo 2010*, Vancouver, Canada, June 2011.

[11] Lang, A., Lecourt, R., and Guliani., F., Statistical evaluation of ignition phenomena in turbojet engines. *Proceedings of ASME Turbo Expo 2010*, Glasgow, June 2010.

[12] Pascaud, S., *Vers la simulation aux grandes échelles des écoulements turbulents diphasiques réactifs : application aux foyers aéronautiques*. PhD Thesis, Université de Toulouse, 2006.

[13] Syred, N., A review of oscillation mechanisms and the role of the precessing vortex core (PVC) in swirl combustion systems. *Progress in Energy and Combustion Science*, 32:93-161.

[14] García Rosa, N., Linassier, G., Lecourt, R., Villedieu, P., Lavergne, G., Experimental and numerical study of high-altitude ignition of a turbojet combustor. *Heat Transfer Engineering*, Xi'an, 2009.

[15] Linassier, G., Lecourt, R., Villedieu, P., Lavergne, G., and Verdier, H., Numerical and experimental study of aircraft engine ignition. *23rd European Conference on Liquid Atomization and Spray Systems*, Brno, Czech Republic, September 2010.

[16] Franzelli, B., Riber, E., Sanjose, M., and Poinsot, T., A two-step chemical scheme for large eddy simulation of kerosene-air flames. *Combustion and Flame*, 157:1364-1373.

[17] Eyssartier, A., Cuenot, B. , Gicquel, L.Y.M. , Poinsot, T., Using les to predict ignition sequences and ignition probability of turbulent two-phase flames, *Combustion and Flame*, *(submitted in june 2011)*, 2012.

[18] Damkohler, G., *NACA TM 1112*, 1947.

[19] Borgi, R., and Champion, M., *Modélisation et théorie des flammes*, Éditions TECHNIP.

[20] Aggarwal, S.K., *Progress in Energy and Combustion Science*, 24:565-600.